

On a soliton-type spacetime defect¹

F R Klinkhamer

Institute for Theoretical Physics, Karlsruhe Institute of Technology (KIT), 76128 Karlsruhe, Germany

E-mail: frans.klinkhamer@kit.edu

Abstract. We review the construction of a particular soliton-type solution of the classical Einstein and matter-field equations. This localized finite-energy static classical solution can be interpreted as a single spacetime defect embedded in Minkowski spacetime and may give rise to several new effects. For a Skyrme-type theory with small enough matter-field energy scale compared to the Planck energy scale and for a sufficiently small defect length scale, the existence of a globally regular solution requires a negative active gravitational mass, so that the defect repels a distant test particle (“antigravity”). There also exist so-called stealth defects (having a positive energy density of the matter fields but a vanishing asymptotic gravitational mass) which bring about a new type of gravitational lensing.

1. Introduction

One hypothesis is that the Universe started out in some form of “quantum phase” which gave rise to classical spacetime and gravity, as described by Einstein’s General Theory of Relativity [1]. It is then possible that this process is analogous to the cooling of a liquid, which produces an atomic crystal. But, if the cooling of the latter process is rapid, the resulting crystal will be imperfect, containing crystallographic defects. For the above-mentioned quantum phase and the resulting classical spacetime, the analogy suggests the possibility of having “spacetime defects” (i.e., imperfections in the fabric of spacetime). Remark that, historically, some of the earliest ideas on a foam-like structure of spacetime go back to Wheeler in the 1950s (cf. Sec. 43.4 and Box 44.3 in Ref. [1] and Chap. 6 in Ref. [2]).

Little is known for sure about the quantum phase of spacetime. Loop quantum gravity, for example, does have something like “atoms of space,” but the emergence of a classical spacetime has not been established (cf. Refs. [3, 4, 5] and references therein).

Here, we will stay on the classical side of the problem and use the framework of Einstein’s General Relativity (GR). Specifically, we will obtain a soliton-type classical solution to describe a single spacetime defect and we will investigate certain novel effects which this soliton-type solution produces.

The aim of the present contribution is to give a more or less self-contained presentation of one particular soliton-type classical solution, namely a Skyrmion spacetime defect solution [6] and to explain the origin of certain new phenomena [7, 8, 9]. In Sec. 2, we first review some background material on the manifold considered (see also Refs. [10, 11, 12, 13]), then define the fields and their action, and, finally, present the details of the Skyrmion spacetime defect

¹ Invited talk at the *Ninth International Workshop DICE2018: Spacetime – Matter – Quantum Mechanics*, Castiglioncello, Tuscany, Italy, September 17–21, 2018. (arXiv:1811.01078)

solution. In Sec. 3, we explain why certain Skyrmion spacetime defects produce “antigravity,” that is, repulsion of a distant test particle. In Sec. 4, we discuss certain Skyrmion spacetime defects which have a positive energy density of the matter fields but a vanishing asymptotic gravitational mass, so that these defects may be called “stealth defects.” In Sec. 5, we show that such stealth defects are not entirely invisible, as they induce lensing of light (this lensing is different from standard gravitational lensing). In Sec. 6, we, first, compare our soliton-type spacetime defect with another type of spacetime defect [14, 15] and, then, review the general properties of the Skyrmion spacetime defect.

Before we start with the technical discussion of the next section, we emphasize that our Skyrmion spacetime defect is a genuine solution of standard GR, as long as we allow for degenerate metrics. The hope is that the equations of GR know about the “edge of the theory” and that they may provide some insight into the nature of possible defects of spacetime.

2. Skyrmion spacetime defect

2.1. Basic idea

Let us start by giving a rough description of our spacetime defect solution [6], with mathematical details to follow later. The basic idea is to obtain a *nonsingular* finite-energy static defect solution of the Einstein field equation, with a length parameter $b > 0$ and topology as suggested by the sketch in Fig. 1.

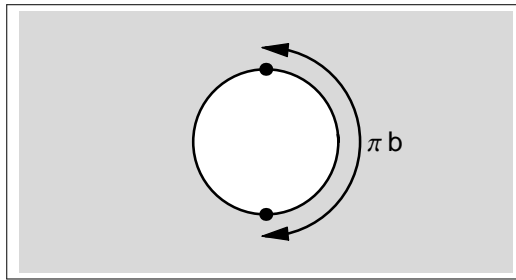


Figure 1. Three-space \widetilde{M}_3 obtained by surgery from the Euclidean 3-space E_3 : interior of a ball with radius b removed and antipodal points on the boundary of the ball identified (as indicated by the dots). The “long distance” between identified points on the defect surface equals πb .

The crucial ingredient of such a regular solution is the choice of *appropriate coordinates*. The standard Cartesian coordinates of Euclidean 3-space are unsatisfactory, as a single point may have different coordinates. Taking the origin of the Cartesian coordinates to coincide with the center of the 3-ball in Fig. 1, the coordinates $(x^1, x^2, x^3) = (0, b, 0)$ and $(x^1, x^2, x^3) = (0, -b, 0)$, for example, correspond to the same point (the identified dots in Fig. 1). Instead of a single chart of Cartesian coordinates, it is possible to use three overlapping charts of coordinates, each one centered on one of the three Cartesian coordinate axes [12, 13]. The promised mathematical details now follow.

2.2. Manifold

The four-dimensional spacetime manifold considered has topology

$$\widetilde{M}_4 = \mathbb{R} \times \widetilde{M}_3, \quad (1)$$

where \widetilde{M}_3 is a noncompact, orientable, nonsimply-connected manifold without boundary. Up to a point, \widetilde{M}_3 is homeomorphic to the 3-dimensional real-projective plane,

$$\widetilde{M}_3 \simeq \mathbb{R}P^3 - p_\infty, \quad (2)$$

where p_∞ corresponds to the “point at spatial infinity.”

For the explicit construction of \widetilde{M}_3 , we perform *local surgery* (Fig. 1) on the 3-dimensional Euclidean space $E_3 = (\mathbb{R}^3, \delta_{mn})$. We start from the standard Cartesian and spherical coordinates on \mathbb{R}^3 ,

$$\vec{x} \equiv |\vec{x}| \hat{x} = (x^1, x^2, x^3) = (r \sin \theta \cos \phi, r \sin \theta \sin \phi, r \cos \theta), \quad (3a)$$

with ranges

$$x^m \in (-\infty, +\infty), \quad r \geq 0, \quad \theta \in [0, \pi], \quad \phi \in [0, 2\pi]. \quad (3b)$$

Now, \widetilde{M}_3 is obtained from \mathbb{R}^3 by removing the interior of the ball B_b with radius b and identifying antipodal points on the boundary $S_b \equiv \partial B_b$. With point reflection denoted $P(\vec{x}) = -\vec{x}$, the 3-space \widetilde{M}_3 is given by

$$\widetilde{M}_3 = \left\{ \vec{x} \in \mathbb{R}^3 : \left(|\vec{x}| \geq b > 0 \right) \wedge \left(P(\vec{x}) \hat{\equiv} \vec{x} \text{ for } |\vec{x}| = b \right) \right\}, \quad (4)$$

where $\hat{\equiv}$ stands for point-wise identification.

As mentioned before, a relatively simple covering of \widetilde{M}_3 uses three charts of coordinates, labeled by $n = 1, 2, 3$. Each chart surrounds one of the three Cartesian coordinate axes, as illustrated by Fig. 2.

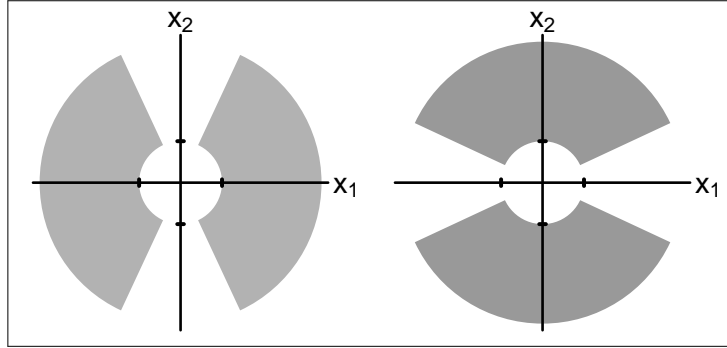


Figure 2. Slice $x_3 = 0$ of the manifold \widetilde{M}_3 with the domains of the chart-1 coordinates (left) and the chart-2 coordinates (right). The tick marks on the x_1 and x_2 axes correspond to the values $\pm b$. The 3-dimensional domains are obtained by revolution around the x_1 -axis (left) or the x_2 -axis (right). The domain of the chart-3 coordinates is defined similarly.

These coordinate charts are denoted

$$(X_n, Y_n, Z_n), \quad \text{for } n = 1, 2, 3. \quad (5)$$

Note that the triples (5) are, despite appearances, non-Cartesian coordinates. Specifically, the set of coordinates surrounding the x^2 -axis segments with $|\vec{x}| \geq b$ is given by (cf. Sec. II D in Ref. [11])

$$X_2 = \begin{cases} \phi, & \text{for } 0 < \phi < \pi, \\ \phi - \pi, & \text{for } \pi < \phi < 2\pi, \end{cases} \quad (6a)$$

$$Y_2 = \begin{cases} +\sqrt{r^2 - b^2}, & \text{for } 0 < \phi < \pi, \\ -\sqrt{r^2 - b^2}, & \text{for } \pi < \phi < 2\pi, \end{cases} \quad (6b)$$

$$Z_2 = \begin{cases} \theta, & \text{for } 0 < \phi < \pi, \\ \pi - \theta, & \text{for } \pi < \phi < 2\pi, \end{cases} \quad (6c)$$

with ranges

$$X_2 \in (0, \pi), \quad Y_2 \in (-\infty, \infty), \quad Z_2 \in (0, \pi). \quad (6d)$$

The two other coordinate sets, (X_1, Y_1, Z_1) and (X_3, Y_3, Z_3) , are defined similarly.

In the following, we explicitly discuss only one coordinate chart, which we take to be (6). Furthermore, the notation is simplified as follows:

$$(X, Y, Z, T) \equiv (X_2, Y_2, Z_2, T), \quad (7)$$

where the time coordinate T has been added in order to describe the spacetime manifold \widetilde{M}_4 .

2.3. Fields and action

Consider a Skyrme-type scalar field $\Omega(X) \in SO(3)$, which propagates over the spacetime manifold (1) and has the following action ($c = \hbar = 1$):

$$S = \int_{\widetilde{M}_4} d^4X \sqrt{-g} \left(\mathcal{L}_{\text{grav}} + \mathcal{L}_{\text{mat}} \right), \quad (8a)$$

$$\mathcal{L}_{\text{grav}} = \frac{1}{16\pi G_N} R, \quad (8b)$$

$$\mathcal{L}_{\text{mat}} = \frac{f^2}{4} \text{tr}(\omega_\mu \omega^\mu) + \frac{1}{16e^2} \text{tr}([\omega_\mu, \omega_\nu] [\omega^\mu, \omega^\nu]) + \frac{1}{2} m^2 f^2 \text{tr}(\Omega - \mathbb{1}_3), \quad (8c)$$

$$\omega_\mu \equiv \Omega^{-1} \partial_\mu \Omega, \quad (8d)$$

where R is the Ricci curvature scalar. With “pions” π^a defined by

$$\Omega(X) = \exp \left[S^a \pi^a(X)/f \right], \quad (9)$$

for 3×3 matrices S^a given by

$$S^1 \equiv \begin{pmatrix} 0 & 0 & 0 \\ 0 & 0 & 1 \\ 0 & -1 & 0 \end{pmatrix}, \quad S^2 \equiv \begin{pmatrix} 0 & 0 & -1 \\ 0 & 0 & 0 \\ 1 & 0 & 0 \end{pmatrix}, \quad S^3 \equiv \begin{pmatrix} 0 & 1 & 0 \\ -1 & 0 & 0 \\ 0 & 0 & 0 \end{pmatrix}, \quad (10)$$

we have

$$\mathcal{L}_{\text{mat}} = -\frac{1}{2} \partial_\mu \pi^a \partial^\mu \pi^a - \frac{1}{2} m^2 \pi^a \pi^a + \dots. \quad (11)$$

The theory (8) has three dimensional parameters and a single dimensionless parameter e ,

$$G_N \geq 0, \quad (12a)$$

$$f > 0, \quad (12b)$$

$$m \geq 0, \quad (12c)$$

$$e > 0. \quad (12d)$$

From these parameters, we obtain the following two dimensionless parameters:

$$\tilde{\eta} \equiv 8\pi G_N f^2 \geq 0, \quad (13a)$$

$$\tilde{m} \equiv \frac{m}{ef} \geq 0. \quad (13b)$$

2.4. Ansätze

The self-consistent *Ansätze* for the metric and the $SO(3)$ matter field are [6]

$$ds^2 \Big|_{\widetilde{M}_4, \text{chart-2}} = -[\mu(W)]^2 dT^2 + (1 - b^2/W) [\sigma(W)]^2 (dY)^2 + W [(dZ)^2 + \sin^2 Z (dX)^2], \quad (14a)$$

$$\Omega(X) = \cos [F(W)] \mathbb{1}_3 - \sin [F(W)] \hat{x} \cdot \vec{S} + (1 - \cos [F(W)]) \hat{x} \otimes \hat{x}, \quad (14b)$$

$$W \equiv b^2 + Y^2, \quad (14c)$$

with a unit 3-vector $\hat{x} \equiv \vec{x}/|\vec{x}|$ from the Cartesian coordinates \vec{x} defined in terms of the chart-2 coordinates X , Y , and Z [see (3), (6), and (7) above]. Note that the sine- F term in (14b) displays the hedgehog behavior, linking the “isospin” dependance of the matter field $\Omega(X)$ to its spatial dependance.

The boundary conditions on the three *Ansatz* functions are:

$$F(b^2) = \pi, \quad F(\infty) = 0, \quad (15a)$$

$$\sigma(b^2) \in (0, \infty), \quad (15b)$$

$$\mu(b^2) \in (0, \infty). \quad (15c)$$

The boundary condition (15a) at $W = b^2$ is consistent with the topology of \widetilde{M}_3 [identified antipodal points in Fig. 1] and the boundary conditions (15b)–(15c) will be discussed later.

Two remarks on these *Ansätze* are in order. First, with finite *Ansatz* functions $\mu(W)$ and $\sigma(W)$, the metric from (14a) is **degenerate** at the defect surface $Y = 0$ (or $W = b^2$):

$$g(X) \Big|_{W=b^2} \equiv \det[g_{\mu\nu}(X)] \Big|_{W=b^2} = 0, \quad (16)$$

and the standard elementary-flatness property does not apply (cf. App. D in Ref. [10]). Further discussion on the degeneracy property is relegated to Sec. 6.2.

Second, the matter-field *Ansatz* (14b) corresponds to a topologically nontrivial scalar field configuration, a Skyrmion-like configuration [16, 17] with **unit winding number**,

$$N \equiv \deg[\Omega] = -\frac{2}{\pi} \int_{\pi}^0 dF \sin^2(F/2) = 1, \quad (17)$$

where the endpoints of the integral correspond to the boundary conditions (15a). Again, further discussion is relegated to Sec. 6.2.

2.5. Reduced field equations

In our numerical analysis, we will use the following dimensionless variables:

$$y \equiv e f Y \in (-\infty, \infty), \quad (18a)$$

$$y_0 \equiv e f b \in (0, \infty), \quad (18b)$$

$$w \equiv (e f)^2 W \equiv y_0^2 + y^2 \in [y_0^2, \infty), \quad (18c)$$

and the *Ansatz* functions are simply written as $F(w)$, $\sigma(w)$, and $\mu(w)$. The reduced field equations are three ordinary differential equations (ODEs). With the auxiliary functions

$$A(w) \equiv 2 \sin^2 \frac{F(w)}{2} \left(\sin^2 \frac{F(w)}{2} + w \right), \quad C(w) \equiv 4 \sin^2 \frac{F(w)}{2} + w, \quad (19)$$

these ODEs are [8, 13]:

$$4w\sigma'(w) = +\sigma(w) \left[[1 - \sigma^2(w)] + \tilde{\eta} \frac{2}{w} \left(A(w) \sigma^2(w) + C(w) [w F'(w)]^2 \right) \right] + 2w\tilde{m}^2 \tilde{\eta} \sigma^3(w) \sin^2 \frac{F(w)}{2}, \quad (20a)$$

$$4w\mu'(w) = -\mu(w) \left[[1 - \sigma^2(w)] + \tilde{\eta} \frac{2}{w} \left(A(w) \sigma^2(w) - C(w) [w F'(w)]^2 \right) \right] - 2w\tilde{m}^2 \tilde{\eta} \sigma^2(w) \sin^2 \frac{F(w)}{2}, \quad (20b)$$

$$\begin{aligned} C(w) w^2 F''(w) = & +\sigma^2(w) \sin F(w) \left(\sin^2 \frac{F(w)}{2} + \frac{w}{2} \right) - \frac{1}{2} C(w) \sigma^2(w) w F'(w) \\ & \times \left[1 - 4\tilde{\eta} \frac{1}{w} \sin^2 \frac{F(w)}{2} \left(\sin^2 \frac{F(w)}{2} + w \right) \right] \\ & - w F'(w) \left[w F'(w) \sin F(w) + w \right] + \frac{\tilde{m}^2}{2} w^2 \sigma^2(w) \sin \frac{F(w)}{2} \\ & \times \left[\cos \frac{F(w)}{2} + 2\tilde{\eta} C(w) \sin \frac{F(w)}{2} F'(w) \right], \end{aligned} \quad (20c)$$

where the prime stands for differentiation with respect to w .

2.6. Matter energy density and gravitational mass

For later use, we also give the reduced expression for the 00-component of the energy-momentum tensor $T^\mu_\nu(w)$ which corresponds to the negative of the energy density $\rho(w)$,

$$\begin{aligned} T^0_0(w) = & -f^2 (e f)^2 \frac{2}{w^2 \sigma^2(w)} \\ & \times \left(A(w) \sigma^2(w) + C(w) [w F'(w)]^2 + \tilde{m}^2 w^2 \sigma^2(w) \sin^2 \frac{F(w)}{2} \right). \end{aligned} \quad (21)$$

The expression in the large brackets on the right-hand side of (21) has already appeared on the right-hand side of (20a), which resulted from the 00-component of the Einstein equation.

A further useful quantity is the dimensionless length $l(w)$, defined by

$$l(w) \equiv \sqrt{w} \left[1 - \frac{1}{\sigma^2(w)} \right], \quad (22)$$

which corresponds to a Schwarzschild-type behavior of the square of the metric function,

$$\sigma^2(w) = \frac{1}{1 - l(w)/\sqrt{w}}. \quad (23)$$

The σ -ODE (20a) gives immediately

$$l'(w) = \tilde{\eta} w^{-3/2} \left(A(w) + C(w) \frac{[w F'(w)]^2}{\sigma^2(w)} \right), \quad (24)$$

where the prime stands for the derivative d/dw and the auxiliary functions $A(w)$ and $C(w)$ are given by (19). As the right-hand-side of (24) is manifestly nonnegative, the interpretation is

that the mass-type variable $l(w)$ can only increase by the addition of positive energy density from the matter fields [7]. The asymptotic value of $l(w)$ defines the Arnowitt–Deser–Misner (ADM) mass in our context,

$$M_{\text{ADM}} = l_{\infty} / (2 G_N e f), \quad l_{\infty} \equiv \lim_{w \rightarrow \infty} l(w), \quad (25)$$

which corresponds to the active gravitational mass of the soliton-type solution [12, 13].

2.7. Numerical solutions

The ODEs (20) can be solved numerically with boundary conditions from (15). Specifically, we have $F(y_0^2) = \pi$ and $F(\infty) = 0$ for the matter-field *Ansatz* function $F(w)$ and we, first, take $\sigma(y_0^2) = 1$ for the metric *Ansatz* function $\sigma(w)$ [the value of $\mu(y_0^2)$ can be rescaled arbitrarily].

Figure 3 shows the *Ansatz* functions $F(w)$, $\sigma(w)$, and $\mu(w)$ of one particular numerical solution. Also displayed are the dimensionless Ricci curvature scalar $R(w)$, the dimensionless Kretschmann curvature scalar $K(w)$, and the negative of the 00 component of the dimensionless Einstein tensor $E^{\mu}_{\nu}(w) \equiv R^{\mu}_{\nu}(w) - (1/2) R(w) \delta^{\mu}_{\nu}$ [note that $-E^0_0(w)$ is proportional to the energy density $\rho(w)$ by the Einstein equation]. This Fig. 3 shows, moreover, the behavior of the dimensionless Schwarzschild-type length scale $l(w)$ defined by (22), which, as mentioned in Sec. 2.6, stays constant or increases with increasing w . All physical quantities are well-behaved at the defect surface $w = y_0^2$, as shown by Fig. 9 in Ref. [7].

The boundary condition $\sigma(y_0^2) = 1$ may be called the “standard” boundary condition, because the limit $b \rightarrow 0$ then connects to the standard Minkowski spacetime manifold. But with $b \neq 0$ and the nontrivial topology $\mathbb{R}P^3$ from (2), the boundary condition on the metric *Ansatz* function can be generalized:

$$\sigma(y_0^2) \in (0, \infty), \quad (26)$$

where the value zero has been excluded, in order that the field equations be well-defined at the $w = y_0^2$ defect surface [13].

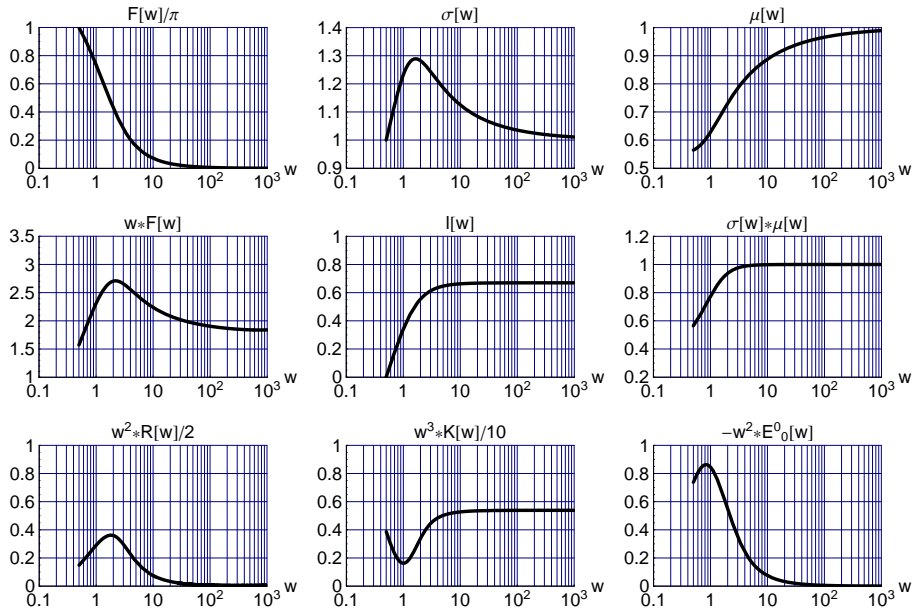


Figure 3. Numerical solution [7] of the reduced field equations (20) with parameters $\tilde{\eta} \equiv 8\pi G_N f^2 = 1/20$, $\tilde{m} \equiv m/(e f) = 0$, and $y_0 \equiv e f b = 1/\sqrt{2}$, and boundary conditions at the defect surface $w = y_0^2 = 1/2$: $F = \pi$, $F' = -1.9718377138$, $\sigma = 1$, and $\mu = 0.564337$.

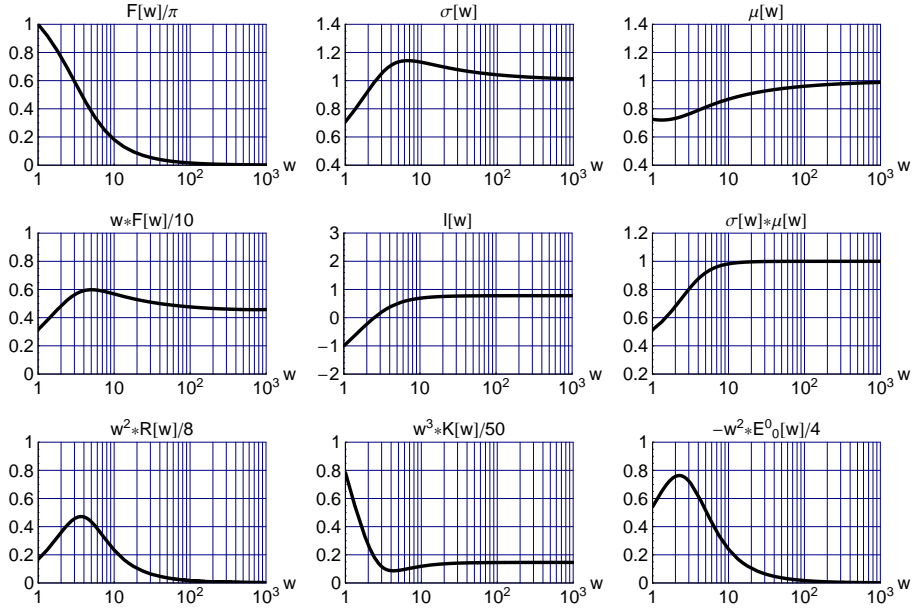


Figure 4. Numerical solution [7] of the ODEs (20) with parameters $\tilde{\eta} = 1/10$, $\tilde{m} = 0$, and $y_0 = 1$, and boundary conditions at $w = y_0^2 = 1$: $F = \pi$, $F' = -0.82561881304$, $\sigma = 1/\sqrt{2}$, and $\mu = 0.725818$. This numerical solution with $l_\infty \sim 0.8$ has a positive ADM mass from (25).

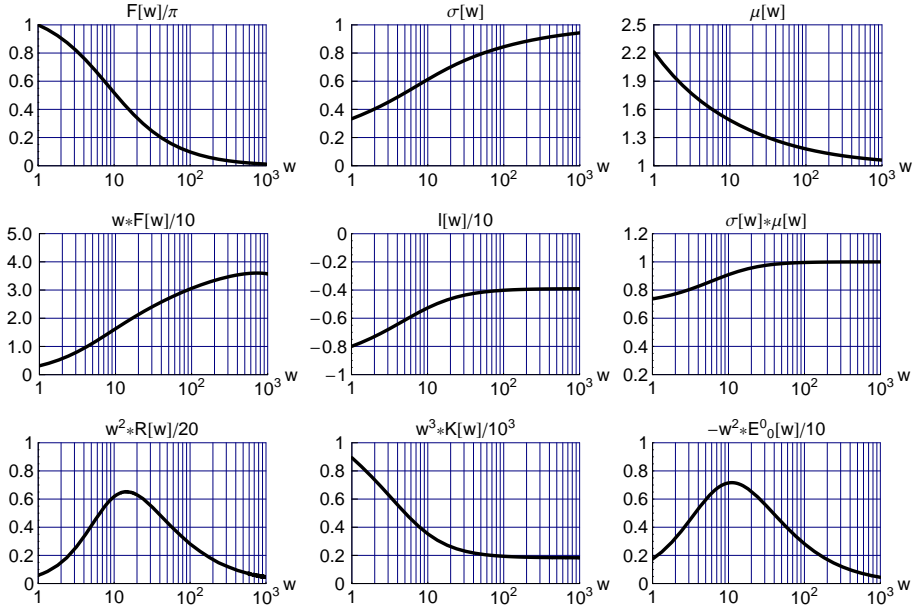


Figure 5. Same as Fig. 4, but now with a smaller value of $\sigma(y_0^2)$. Specifically, the boundary conditions at $w = y_0^2 = 1$ are: $F = \pi$, $F' = -0.323978148$, $\sigma = 1/3$, and $\mu = 2.21176$. This numerical solution with $l_\infty \sim -4$ has a negative ADM mass from (25).

Figures 4 and 5 give numerical solutions for two different values of $\sigma(y_0^2) < 1$. The results of Figs. 3–5 are to be understood as having *different* values of the boundary condition $\sigma(y_0^2)$ for *equal* boundary conditions $F(y_0^2) = \pi$ and $F(\infty) = 0$ [the numerical values for $F'(y_0^2)$ in the figure captions are mentioned purely for technical reasons, as the numerical solutions are easier to obtain with all boundary conditions at one side, $w = y_0^2$]. The qualitative behavior of the $\sigma(w)$ curves in these figures changes: the $\sigma(w)$ curves of Figs. 3 and 4 approach unity from above as $w \rightarrow \infty$ [resulting in $M_{\text{ADM}} > 0$, according to (23) and (25)], while the $\sigma(w)$ curve of Fig. 5 approaches unity from below as $w \rightarrow \infty$ [resulting in $M_{\text{ADM}} < 0$].

3. Antigravity

3.1. Origin of a new phenomenon

Any localized object made of ponderable matter (e.g., quarks and leptons of the Standard Model) **attracts** a distant test particle. This phenomenon is called **gravity** and was first studied by Newton in his *Principia* [1687].

With the solution of Fig. 5, we have a localized object which **repels** a distant test particle. The phenomenon may be called “**antigravity**.” The crucial ingredients of this particular object are, in the framework of Einstein’s General Relativity [1915], the nontrivial topology of space [here, $\mathbb{R}P^3$] and the nontrivial gravitational fields at the defect surface [here, $\sigma(b^2) < 1$ for the *Ansatz* (14a)].

Figures 4 and 5 suggest that the Skyrmion spacetime defect can have either a positive or a negative gravitational mass, but we have a further result: *a sufficiently small defect solution exists only if it has a negative gravitational mass* [a more precise formulation will be given later].

Consider, first, the nature of the solutions with “standard” boundary condition $\sigma(b^2) = 1$. It is, then, found that the solution collapses if it becomes too small (loosely speaking, if b is of the order of or less than the effective Schwarzschild radius); see Fig. 6 for numerical results at one particular value of the coupling constant $\tilde{\eta}$. There is then a *critical curve* in the $(b, \tilde{\eta})$ plane, above which there are no globally regular solutions with $\sigma(b^2) = 1$; see Fig. 7 for a numerical approximation of this critical curve.

Let us now discuss the heuristics for obtaining an anti-gravitating spacetime defect. In order to get a globally regular solution in the region *above* the critical curve of Fig. 7, we need to add a sufficiently negative effective mass at the defect surface ($y = 0$). Now, the dimensionless effective mass is given by (22) with $w \equiv y_0^2 + y^2$. Then, $l(y_0^2) < 0$ results from $\sigma(y_0^2) < 1$.

For a fixed positive value of $\tilde{\eta} \equiv 8\pi G_N f^2$, a sufficiently small globally regular defect solution thus requires a sufficiently negative effective mass at the defect surface $w = y_0^2$ from a nonstandard boundary condition on one of the metric functions, a positive value of $\sigma(y_0^2)$ sufficiently far below unity. For a small enough value of the coupling constant $\tilde{\eta}$, this boundary condition at the defect surface directly gives a negative ADM mass at spatial infinity [see (24) with a near-zero right-hand-side from $\tilde{\eta} \sim 0$ and the definition (25) of M_{ADM}].

3.2. Antigravity from a Planck-scale defect

Let us now give an explicit example [7] of a negative-gravitational-mass Skyrmion spacetime defect. With ζ a number of order 1 or larger, the model parameters are taken as follows:

$$f^2 \ll (E_{\text{planck}})^2 \equiv 1/(8\pi G_N) \approx (2.44 \times 10^{18} \text{ GeV})^2, \quad (27a)$$

$$e \leq 1/\zeta, \quad (27b)$$

where the first inequality corresponds to $\tilde{\eta} = (f/E_{\text{planck}})^2 \ll 1$. The defect is considered to be

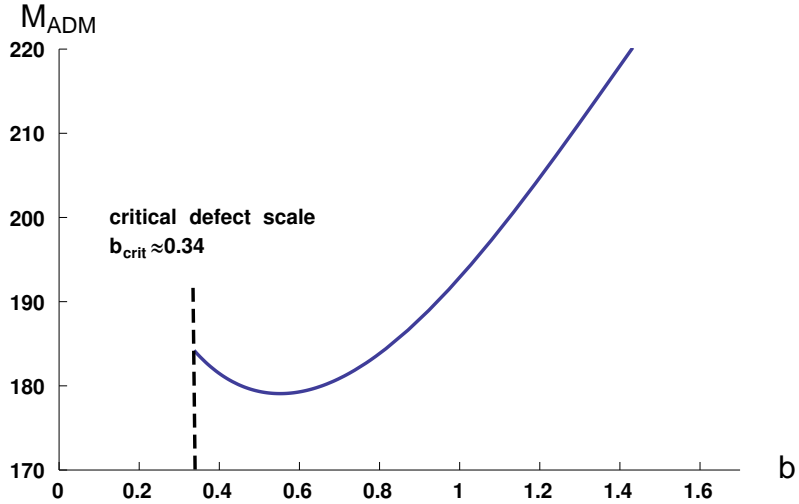


Figure 6. Gravitational mass M_{ADM} [in units f/e] vs. defect scale b [in units $1/(ef)$] from the numerical solutions [7] of the ODEs (20) with boundary condition $\sigma(b^2) = 1$, for parameters $\tilde{\eta} = 0.033$ and $\tilde{m} = 0$.

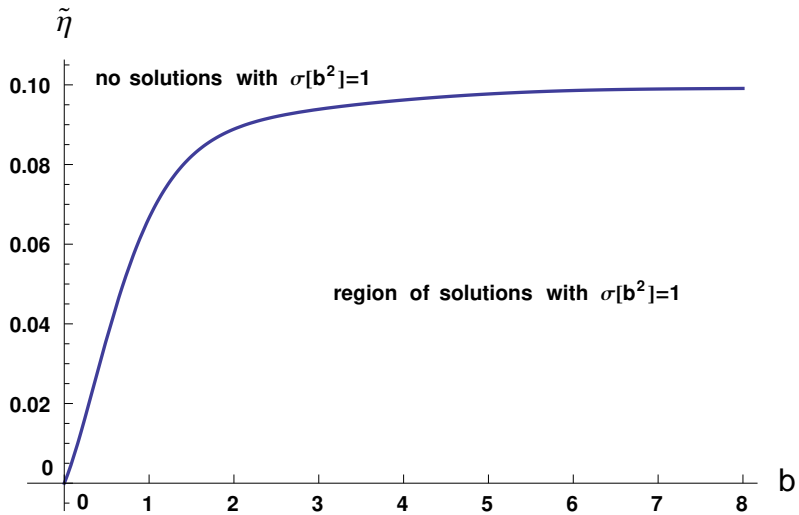


Figure 7. Curve of the critical defect scale b_{crit} [in units of $1/(ef)$] and the corresponding critical coupling constant $\tilde{\eta}_{\text{crit}}$, obtained from the numerical solutions [7] of the ODEs (20) with boundary condition $\sigma(b^2) = 1$ and model parameter $\tilde{m} = 0$.

a remnant of a quantum-spacetime phase and the defect scale is given by

$$b_{\text{remnant}} = \zeta l_{\text{planck}}, \quad (28a)$$

$$l_{\text{planck}} \equiv \sqrt{8\pi G_N \hbar/c^3} \approx 8.10 \times 10^{-35} \text{ m}, \quad (28b)$$

with $\zeta \gtrsim 1$.

The bounds (27) and the defect scale (28) imply that the solution corresponds to a point above the critical curve of Fig. 7, so that a negative effective mass at the defect surface is required in order to prevent gravitational collapse. The resulting defect mass [from (25) with $l_\infty \sim -1$]

is then

$$M_{\text{ADM}} \sim -\frac{4\pi}{\tilde{\eta}} \frac{f}{e} = -\left(\frac{4\pi}{e}\right) \left(\frac{E_{\text{planck}}}{f}\right) E_{\text{planck}}. \quad (29)$$

According to the inequalities (27a) and (27b), the absolute value $|M_{\text{ADM}}|$ from (29) typically is much larger than $E_{\text{planck}} \approx 4.34 \times 10^{-6}$ g.

4. Stealth defect

We have seen that certain soliton-type defect solutions can have positive gravitational mass but also negative gravitational mass. As the gravitational mass of such a spacetime-defect solution is a continuous variable, there must be special spacetime defects with vanishing gravitational mass. These defects with positive energy density of the matter fields and zero asymptotic gravitational mass will be called “stealth defects” [8]. An explicit solution with vanishing gravitational mass and an exponentially-vanishing energy density of the matter fields is given in Fig. 8.

Now, assume that all matter fields have some form of non-gravitational interaction with each other. If so, there will, in principle, be some interaction between the “pions” of the theory considered in (8) and the elementary particles of the Standard Model. Then, consider what happens with a head-on collision of a stealth defect and a human observer made of Standard Model particles (mostly up and down quarks, gluons, and electrons). In close approximation, the observer will have no idea of what is going to happen, until he/she is within a distance of order $h/(mc)$ from the defect, where m is the “pion” mass scale from the matter action (8c). What happens during the collision itself and afterwards depends on the details of the setup, for example, the size of the observer compared to the defect scale b .

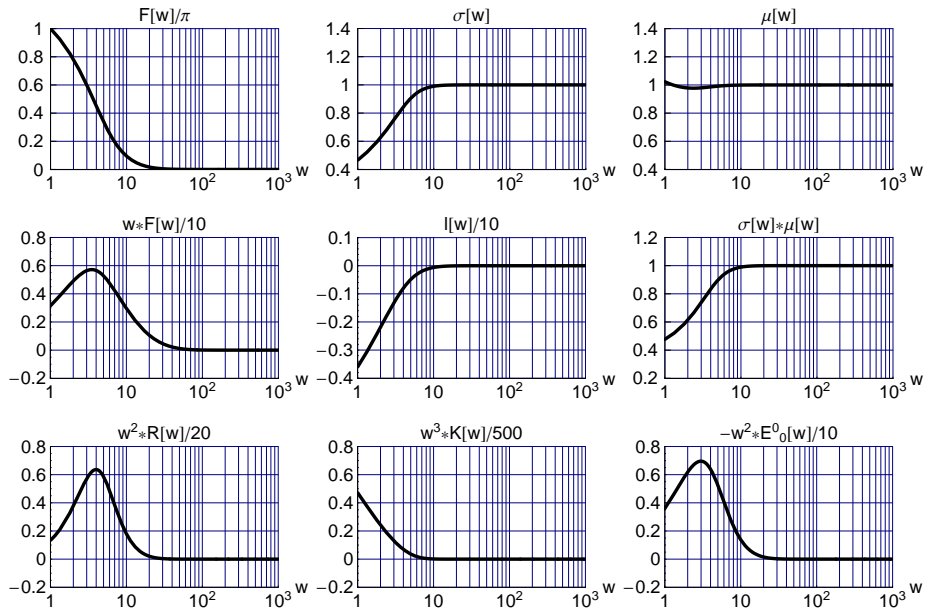


Figure 8. Numerical solution [8] of the ODEs (20) with parameters $\tilde{\eta} = 1/10$, $\tilde{m} = 1$, and $y_0 = 1$. The boundary conditions at $w = 1$ are: $F/\pi = 1.00000$, $F' = -0.752388$, $\sigma = 0.466343$, and $\mu = 1.02282$. The value of $|l(10^3)|$ is less than 10^{-11} , which gives an essentially vanishing ADM mass (25).

5. Lensing by a stealth defect

Consider the behavior of light rays propagating over a spacetime-defect manifold. It is, in fact, possible to give a simplified discussion [9] by use of an exact vacuum solution [10]:

$$ds^2 \Big|_{\widetilde{M}_4, \text{chart-2}}^{(\text{vac. sol.})} = - \left(1 - \widehat{l}/\sqrt{w}\right) (dt)^2 + \frac{1 - y_0^2/w}{1 - \widehat{l}/\sqrt{w}} (dy)^2 + w \left[(dz)^2 + \sin^2 z (dx)^2\right], \quad (30a)$$

$$w \equiv y_0^2 + y^2, \quad y_0 \equiv e f b > 0, \quad \widehat{l} \in (-\infty, y_0). \quad (30b)$$

In the notation of (14a), we have $[\mu(w)]^2 = 1/[\sigma(w)]^2 = 1 - \widehat{l}/\sqrt{w}$. In our setup, the vacuum metric (30) can arise in two ways: first, from the solution of Sec. 2 with nontrivial matter-field boundary conditions (15a) in the limit $G_N \rightarrow 0$ for fixed energy scale $f > 0$ or, second, from the metric of Sec. 2 with a trivial matter field $F(W) = 0$, so that the matter energy density (21) vanishes identically.

Next, consider the special case of a stealth-defect vacuum solution with

$$\widehat{l} = 0, \quad (31)$$

which has a flat spacetime with vanishing curvature scalars, $R(w) = K(w) = 0$. We consider this “extreme” case, in order to emphasize the difference with standard gravitational lensing [18] which is due to the curvature of spacetime resulting from a nonvanishing matter distribution.

Remark that *exact* multi-defect solutions of the vacuum Einstein equation can be obtained by superposition of these static $\widehat{l} = 0$ defects, provided the individual defect surfaces do not intersect. The resulting “gas” of static defects violates Lorentz invariance. In principle, we can also obtain an exact multi-defect solution of the vacuum Einstein equation which is approximately Lorentz invariant, if we superpose quasi-randomly positioned and quasi-randomly moving $\widehat{l} = 0$ defects (arranged to be nonintersecting initially).

Returning to the single $\widehat{l} = 0$ defect (30), the geodesics are readily calculated:

- straight lines in the ambient Euclidean 3-space, if there are no intersections with the defect surface;
- matching straight-line segments in the ambient Euclidean 3-space, if there are intersections with the defect surface.

Figure 9 gives an example of a geodesic staying away from the defect surface, while Figs. 10 and 11 show geodesics crossing the defect surface, with or without a parallel shift of the straight-line segments in the ambient Euclidean 3-space (the solid line in Fig. 11, for example, has a parallel shift but the dot-dashed line not).

Due to the parallel shifts at the defect surface, there is a lensing effect, as shown in Fig. 12. This lensing of the flat-spacetime defect results in image formation, as illustrated by Fig. 13.

A few remarks are in order:

- (i) The image in Fig. 13 is located at the reflection point on the other side of the defect.
- (ii) The image is inverted and the image size is equal to the object size. Note that this is also the case if an object in Minkowski spacetime is located at a $2f$ distance from a thin double-convex lens, where f is the focal length of the lens.
- (iii) The irradiance of the image (defined as the power per unit receiving area) depends on the defect scale b and the location of the object: the irradiance of the image will be larger if b is increased for unchanged object position or if the object is brought closer to the defect for unchanged b .
- (iv) If a permanent pointlike light source is placed at point P of Fig. 12, then an observer at point P' in the same figure will see a *luminous disk* (different from the *Einstein ring* [18] which the observer would see if the defect were replaced by a patch of Minkowski spacetime with a static spherical star at the center).

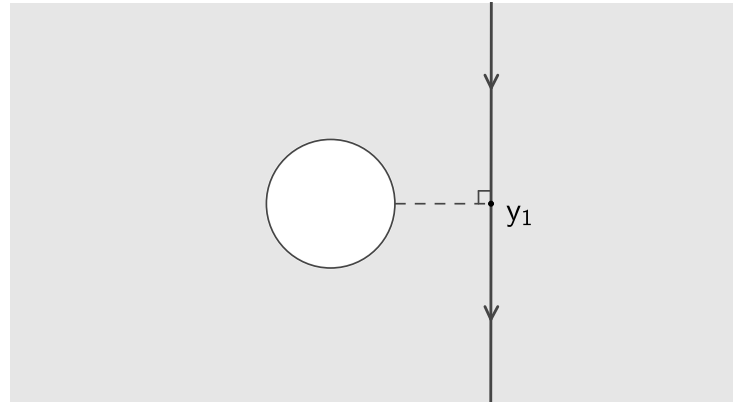


Figure 9. Geodesic which does not cross the defect surface, with part of the 3-space manifold (30)–(31) indicated by the shaded area. The dimensionless quasi-radial coordinate y_1 corresponds to an “impact parameter.”

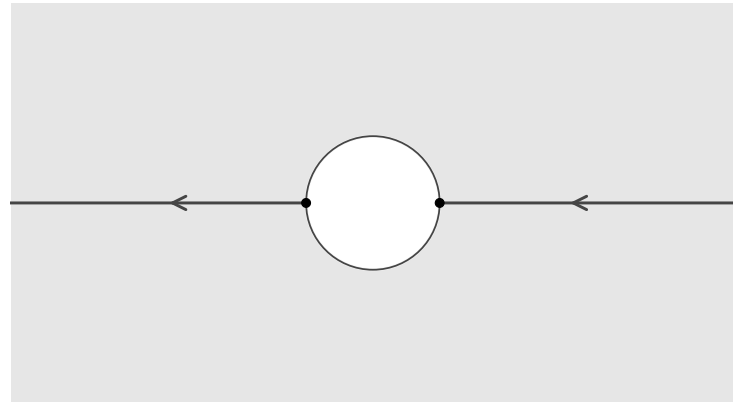


Figure 10. Radial geodesic which crosses the defect surface, where antipodal points (dots) on the defect surface are identified (cf. Fig. 1).

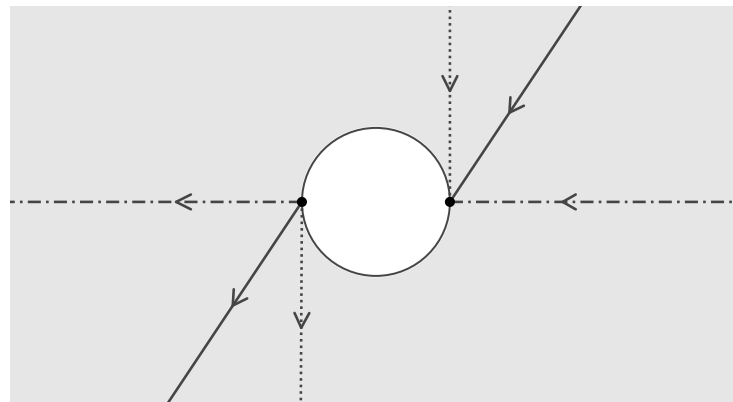


Figure 11. A family of geodesics crossing the defect surface.

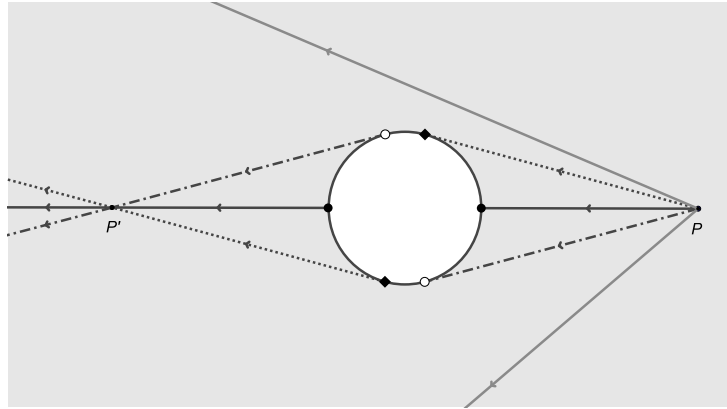


Figure 12. Geodesics with intersection points P and P' .

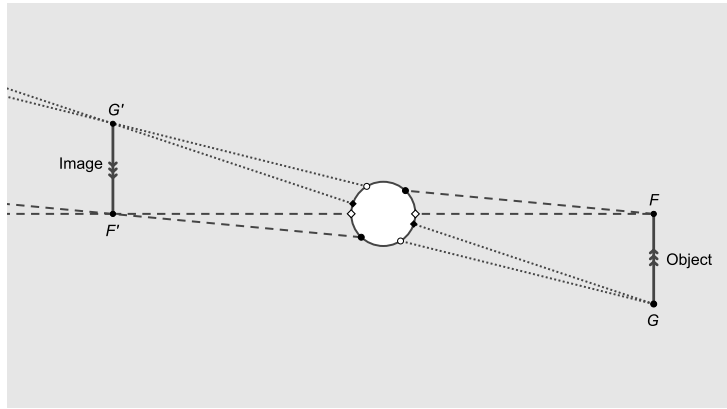


Figure 13. Image formation by the stealth defect.

6. Discussion

Before we review the main characteristics of our soliton-type spacetime defect, we wish to compare our approach to another approach which is more or less orthogonal.

6.1. Comparison to another type of spacetime defect

It is, in principle, possible to define a local spacetime defect not by what it *is* but rather by what it *does*. Precisely this approach has been followed in Refs. [14, 15], where the effect considered is the violation of energy-momentum conservation. More precisely, a single particle moves in the ambient spacetime (i.e., the smooth spacetime away from the localized defect) and is arranged to “collide” with a pointlike spacetime defect, which randomly changes the 4-momentum of the particle. The problem with this approach is how to implement it into a consistent theory (without knowing the details of the defect).

In the flat-spacetime model of Ref. [14], the suggestion is to modify the gauge-covariant derivative appearing in the Lagrange density. But, then, gauge invariance is violated, which will introduce an unacceptable violation of unitarity for the particles in the ambient spacetime.

In the curved-spacetime model of Ref. [15], the usual Levi-Civita connection is modified by the addition of a rank-3 tensor $Q_{\mu\nu}^\lambda = Q_{\nu\mu}^\lambda$, which is thought to be defined on a discrete set of spacetime points (corresponding to the pointlike spacetime defects). The problem, now, is to obtain the modified Einstein equation, which somehow involves derivatives of $Q_{\mu\nu}^\lambda$, even though these $Q_{\mu\nu}^\lambda$ are only defined on a discrete set of points. It is perhaps possible to consider some

smeared-out version of $Q_{\mu\nu}^\lambda$, but this is not really satisfactory for a fundamental theory.

Another possibility is to view the model of Ref. [15] as an effective theory, provided the pointlike defects are replaced by finite-size soliton-type defects. Instead of static soliton-type defects, we then need genuine time-dependent solutions of the classical field equations. Alternatively, we may consider our Skyrmion spacetime defect as a first approximation, where the defect size is considered to be time-dependent: $b = b(t)$ with an approximately constant value $b(t) \sim b_c > 0$ for $|t| < \Delta t$ and an approximately vanishing value $b(t) \sim 0^+$ for $|t| > \Delta t$. This last suggestion for $b(t)$ would correspond to “topology change without topology change” (cf. Sec. 6.6.4 in Ref. [2]). The issue of topology change will also be discussed in Sec. 6.2.

Expanding on the last paragraph, we remark that it is possible to *calculate* the scattering of a “pion” [as defined in (9)] by our $SO(3)$ Skyrmion spacetime defect and to obtain the recoil of the defect. The crucial observation is that our Skyrmion spacetime defect has a finite-width shell of nonvanishing pion-density, as follows from setting $F(w) \sim \pi$ in (21) for w values between y_0^2 and $y_0^2 + (\Delta y)^2$. This finite matter-density shell then scatters a single incoming “pion.” In fact, pion-nucleon scattering [19, 20] has been discussed for the standard $SU(2)$ Skyrmion in Minkowski spacetime and the recoil of this Skyrmion (a finite matter-density ball) has been obtained in Ref. [21, 22]. A similar calculation of the recoil would appear to be feasible for our $SO(3)$ Skyrmion spacetime defect (a finite matter-density shell). This calculated recoil would then provide an explicit realization for the energy-momentum change of the incoming particle (here, a “pion”) as discussed in Ref. [15].

6.2. Remarks on the Skyrmion spacetime defect

The following general remarks aim to put our Skyrmion spacetime defect solution in perspective. First, the new type of Skyrmion solution is rather interesting by itself, as it combines the nontrivial topology of spacetime with the nontrivial topology of field-configuration space. Indeed, the nontrivial topology of the underlying space manifold allows the internal $SO(3)$ space to be covered only once, $N = 1$ in (17).

Second, it remains to be proved that the solution obtained is stable. The scalar fields by themselves would be stable because of the topological charge $N = 1$, but, in principle, there could be still more branches of solutions with even lower values of the ADM mass (the two known branches are shown in Fig. 2 of Ref. [7]).

Third, the Skyrmion-spacetime-defect metric from (14) is degenerate: $\det g_{\mu\nu} = 0$ at the defect surface $Y = 0$, which corresponds to a submanifold $\mathbb{R}P^2 \sim S^2/\mathbb{Z}_2$ (cf. Fig. 1). A heuristic argument for the necessity of a degenerate metric is as follows: the submanifold $\mathbb{R}P^2$ cannot be differentially embedded in \mathbb{R}^3 and this fact implies that a nonsingular solution requires a vanishing metric component g_{YY} at $Y = 0$, making for a vanishing determinant at $Y = 0$ (more details can be found in the third remark of Sec. VI in Ref. [7]).

Fourth, this degenerate metric makes that the Gannon singularity theorem [23] and the Schoen–Yau positive-mass theorem [24] are not directly applicable; we refer to Sec. 3.1.5 in Ref. [13] for further discussion. The special feature of the Skyrmion spacetime defect solution is that certain geodesics at the $\mathbb{R}P^2$ defect surface cannot be continued uniquely: compare the full curve of Fig. 9 in the limit of $y_1 \rightarrow 0^+$ with the dotted curve of Fig. 11.

Fifth, the negative ADM mass found for a small enough defect scale b (at a given value of $\tilde{\eta}$) is not due to ponderable matter but to the nontrivial gravitational fields at the $\mathbb{R}P^2$ defect surface with area $2\pi b^2$. Specifically, the boundary value $\sigma(b^2) \in (0, 1)$ determines the approach to zero of the metric component g_{YY} , according to the metric *Ansatz* (14a).

Sixth, having a negative-gravitational-mass spacetime defect [notably a vacuum solution (30a) with $\hat{l} < 0$] prompts us to reconsider the stability of Minkowski spacetime, especially as classical topology change appears to be possible if degenerate metrics are allowed [25].

Seventh, the crucial open question is the origin and role of nontrivial spacetime topology. For our Skyrmiон spacetime defect solution, two specific questions are:

- (i) what sets the constant defect scale b ?
- (ii) can the defect scale b become a dynamic variable?

There are, of course, many further questions, such as what happens if two defects collide?

The two specific questions listed in the last remark have also been raised in the penultimate paragraph of Sec. 6.1. The issue of (genuine or effective) topology change is crucial for a proper understanding of the small-scale structure of spacetime, which brings us back to the “quantum phase” of the first sentence in Sec. 1.

Acknowledgments

The author thanks the organizers of this interesting workshop, in particular Hans-Thomas Elze. He also thanks J.M. Queiruga and Z.L. Wang for useful comments on the manuscript.

References

- [1] Misner C W, Thorne K S and Wheeler J.A. 2017 *Gravitation* (Princeton NJ: Princeton University Press)
- [2] Visser M 1995 *Lorentzian Wormholes: From Einstein to Hawking* (New York NY: Springer)
- [3] Ashtekar A and Lewandowski J 1997 Quantum theory of geometry. 1. Area operators *Class. Quant. Grav.* **14** A55 (Preprint arXiv:gr-qc/9602046)
- [4] Ashtekar A and Lewandowski J 1998 Quantum theory of geometry. 2. Volume operators *Adv. Theor. Math. Phys.* **1** 388 (Preprint arXiv:gr-qc/9711031)
- [5] Rovelli C 2008 Loop quantum gravity *Living Rev. Rel.* **11** 5
- [6] Klinkhamer F R 2014 Skyrmiон spacetime defect *Phys. Rev. D* **90** 024007 (Preprint arXiv:1402.7048)
- [7] Klinkhamer F R and Queiruga J M 2018 Antigravity from a spacetime defect *Phys. Rev. D* **97** 124047 (Preprint arXiv:1803.09736)
- [8] Klinkhamer F R and Queiruga J M 2018 A stealth defect of spacetime *Mod. Phys. Lett. A* **33** 1850127 (Preprint arXiv:1805.04091)
- [9] Klinkhamer F R and Wang Z L 2019 Lensing and imaging by a stealth defect of spacetime *Mod. Phys. Lett. A* **34** 1950026 (Preprint arXiv:1808.02465)
- [10] Klinkhamer F R 2014 A new type of nonsingular black-hole solution in general relativity *Mod. Phys. Lett. A* **29** 1430018 (Preprint arXiv:1309.7011)
- [11] Klinkhamer F R and Sorba F 2014 Comparison of spacetime defects which are homeomorphic but not diffeomorphic *J. Math. Phys.* **55** 112503 (Preprint arXiv:1404.2901)
- [12] Schwarz M 2010 Nontrivial spacetime topology, modified dispersion relations, and an $SO(3)$ -Skyrme model *PhD Thesis, Karlsruhe Institute of Technology* (Munich, Germany: Verlag Dr. Hut) [ISBN 9783868536232]
- [13] Guenther M 2017 Skyrmiон spacetime defect, degenerate metric, and negative gravitational mass *Master Thesis, Karlsruhe Institute of Technology* [<https://www.itp.kit.edu/en/publications/diploma>]
- [14] Hossenfelder S 2013 Phenomenology of space-time imperfection. II. Local defects *Phys. Rev. D* **88** 124031 (Preprint arXiv:1309.0314)
- [15] Hossenfelder S and Gallego Torromé R 2018 General relativity with space-time defects *Class. Quant. Grav.* **35** 175014 (Preprint arXiv:1709.02657)
- [16] Skyrme T H R 1961 A nonlinear field theory *Proc. Roy. Soc. A* **260** 127
- [17] Manton N S and Sutcliffe P 2004 *Topological Solitons* (Cambridge, UK: Cambridge University Press)
- [18] Schneider P, Ehlers J and Falco E E 1992 *Gravitational Lenses* (Berlin: Springer-Verlag)
- [19] Hayashi A, Eckart G, Holzwarth G and Walliser H 1984 Pion nucleon scattering phase shifts in the Skyrme model *Phys. Lett. B* **147** 5
- [20] Mattis M P and Peskin M E 1985 Systematics of πN scattering in chiral soliton models *Phys. Rev. D* **32** 58
- [21] Uehara M, Hayashi A and Saito S 1991 Meson-soliton scattering with full recoil in standard collective coordinate quantization *Nucl. Phys. A* **534** 680
- [22] Hughes J and Mathews G J 1992 Skyrmiон recoil in pion nucleon scattering *Phys. Rev. D* **46** 970
- [23] Gannon D 1975 Singularities in nonsimply connected spacetimes *J. Math. Phys.* **16** 2364
- [24] Schoen R and Yau S T 1979 On the proof of the positive mass conjecture in general relativity *Commun. Math. Phys.* **65** 45
- [25] Horowitz G T 1991 Topology change in classical and quantum gravity *Class. Quant. Grav.* **8** 587